Proc. Natl. Sci. Counc. ROC(A)
Vol. 21, No. 5, 1997. pp. 416-427

A Multispectral Imaging Spectrometer with Programmable Wavebands

WEI-SONG LIN, CHI-PEI HWANG, AND YI-REN SU

Institute of Electrical Engineering
National Taiwan University
Taipei, Taiwan, R.O.C.

(Received September 4, 1996; Accepted April 12, 1997))

ABSTRACT

Investigation of the spectral signatures of real objects in the field can aid selection of wavebands for remote sensing experiments and can facilitate interpretation of the results. This research focused on developing a multispectral imaging spectrometer for this purpose. The implemented spectral range of detection is from 400 nm to 900 nm, covering visible and near infrared light. To allow freedom in choosing the bandwidths and number of wavebands for various applications, the wavebands are made programmable. An area CCD (Charge Coupled Device) detector with 256×1024 pixels, a 16-bit analog to digital converter, and a pushbroom scanning mechanism enable the system to detect the radiance of an object in one intensive, one spectral and two spatial dimensions. In the extreme case of imaging, 1024 wavebands, 0.1 nm bandwidth, 16-bit resolution of intensity, and a 10 cm square footprint on the object plane can be achieved. The hardware consists of a monochromator, an CCD camera, a light source, an X-stage and a processing unit, which are successfully integrated to perform spectral imaging functions. During operation, the system is supervised by operating software, which is designed to automate the imaging procedures. The resulting spectral data can be saved on a hard disk for further study. For immediate display of the spectral images, gray-scale, 16-color and artificial RGB-color schemes are provided to enhance the presentation. For the sake of testing and demonstration, the spectral characteristics of a geometric pattern and a leaf samples have been investigated by using this imaging spectrometer. Its capability in observing objects using six OCI wavebands has been demonstrated as well. The results show that the goal of the design has been successfully implemented.

Key Words: imaging spectrometer, spectral signature, remote sensing

I. Introduction

When electromagnetic waves are used for remote sensing, surface units and geological or biological materials, can be separated, classified, and identified based upon their spectral signatures. For pure materials, the spectral signature is considered to be some unique characteristic in the reflectivity or emisivity spectrum, such as a diagnostic absorption band or a combination of absorption bands, a diagnostic reflectivity change at a certain wavelength, or the ratio of the reflectivity in two separate spectral regions (Elachi, 1987). High resolution radiometric measurements over a fairly broad region of the spectrum can provide information needed to find spectral signatures. However, the difficulty in identifying objects in the field is the varying composition of geological materials and the mixture of biological materials with underlying materials. Therefore, the spectral features obtained from an area of interest of a sample object constitutes the basic information needed to design a remote sensing experiment and to interpret the data. Laboratory spectroscopic arrangements for observing the spectral signatures of sample objects can be classified into reflection, emission and absorption (or transmittance) types. The major considerations are the wavelength range, the type of physical phenomenon and the design of the observation system. Practical implementations vary in light sources, dispersing elements, and detecting devices. Buschmann *et al.* (1994) developed a spectrometer called VIRAF (Visible Infrared Reflectance Absorptance Fluorescence) for ground truth measurements of vegetation. It is capable of obtaining spectra of reflectance, absorptance, and fluorescence in the visible and near-infrared range (400-910 nm). Pomeroy *et al.* (1995) developed a CCD-based system that uses fiber-optic inputs, which results in a spectroscopic system capable of carrying out both absorption and fluorescence measurement. The individual fiber channels are resolved spatially based on the two-dimen-

sional imaging capabilities of the area array CCD. Using filters, Ning *et al.* (1995) implemented an imaging fluorometer for measurement of the fluorescence signals of plant leaves. This paper proposes a design for and implementation of a multispectral imaging spectrometer for observing the spectral characteristics of sample objects in the visible and near infrared range (400-900 nm). Spectral imaging is carried out using an area CCD detector and a pushbroom scanning mechanism. The wavebands of interest are programmable. In the extreme case, 1024 wavebands, 0.1 nm bandwidth, 16-bit resolution of intensity, and a 10 cm square footprint on the object plane can be achieved. Test results of the system for observation of two sample objects will be given.

The remainder of this paper is organized as follows: Section II describes the architecture of the spectral imaging system, Section III proposes a design for the operating software, Section IV gives the results of experiments on observing a geometric pattern and a leaf sample, and Section V is the conclusion.

II. The Multispectral Imaging Spectrometer

1. Architecture of the Multispectral Imaging Spectrometer

The multispectral imaging spectrometer is composed of a monochromator, a CCD camera, an X-stage, a white light source and a processing unit as shown in Fig. 1. Figure 2 depicts the working environment of the system. The whole system can be divided into four parts. The monochromator and CCD camera are responsible for dispersing and detecting the incoming radiation. The X-stage and its motion controller (computer) form one of the two dimensions of the pushbroom scanning mechanism. The white light source mimics the situation of illumination in passive remote sensing. The processing unit is responsible for the system control, including scanning and data processing. The operating software, which operates under WINDOWS-95, is designed to automate the spectral imaging procedure. The user can simply set up the experimental conditions and then acquire the spectral images of the tested object. Gray-scale, 16-color, and artificial RGB-color schemes have been developed to enhance the presentation of spectral images for immediate investigation.

2. The Monochromator

A monochromator, *MultiSpec 257* from Oriel Co.

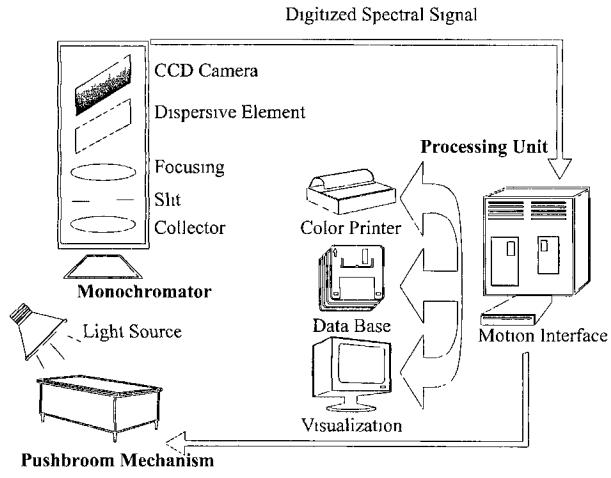

Fig. 1. Architecture of the multispectral imaging spectrometer.

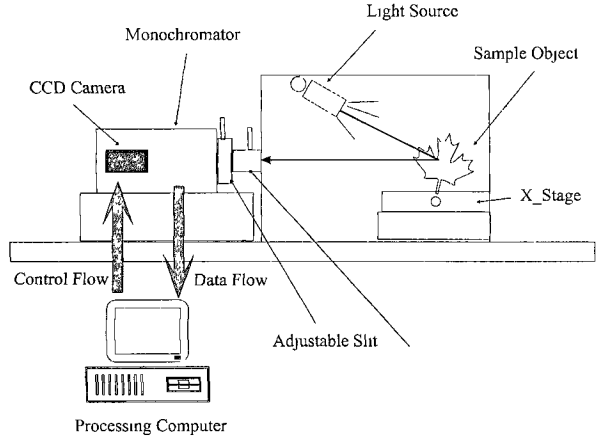

Fig. 2. Working environment of the system.

(Oriel, 1994), is used to disperse incoming radiation into many colored rays. It has a focal length of 257 mm. The complete layout scheme is shown in Fig. 3. The gratings, rapid motor drive, and concave lens are basically optical light-dispersing elements. The integrated shutter, adjustable focus lens, and micrometer slits are used to control the amount of light. The built-in microprocessor board is the main control unit of the monochromator, and two detector ports are supported. The communications interface is the main element for communication with other components. The wiring which connects this device with a computer is shown in Fig. 4.

To provide the function of waveband programmability, two gratings instead of filters are used and set up on a grating turret to disperse the radiation. The two gratings are 1200 lines/mm blazing at 700 nm and 300 lines/mm blazing at 400 nm, respectively. The

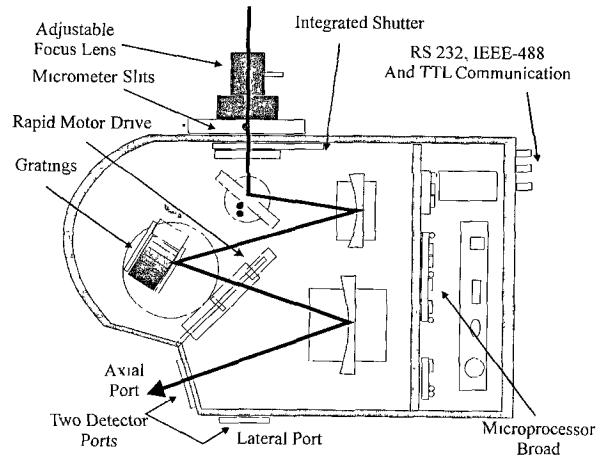

Fig. 3. Layout of the MultiSpec 257 monochromator (Oriel, 1994).

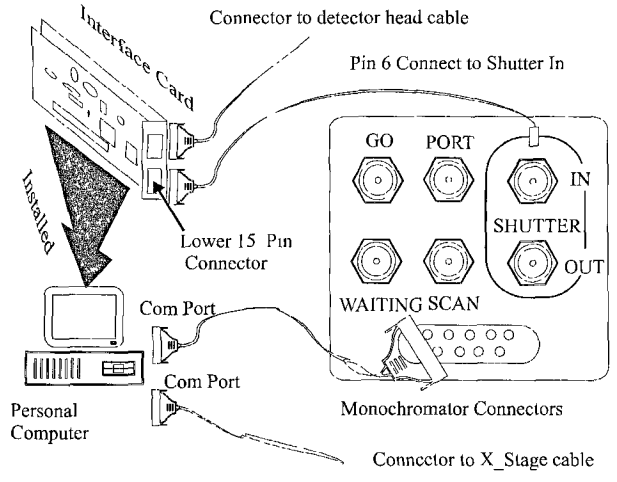

Fig. 4. The wiring between the computer and the monochromator.

grating turret can be rotated by the rapid motor drive. The blaze wavelength is the wavelength at which the most energy is dispersed. The best efficiency we can expect for a grating at the blaze wavelength is about 80%. The blazing wavelength should be set at the extreme short wavelength end of the region of interest because the CCD detector is more sensitive at longer wavelengths.

The mechanical shutter can be used to block the radiation for dark current measurement or to control the exposure. The slit is the major device used to control the amount of incoming radiation. The width of the slit is adjustable with micrometer resolution. The focus lens is a convex lens used to project the image onto the slit plane. In our design, the convex lens has a focus of 32 mm. A standard RS-232 communication interface is used to receive commands from the computer.

3. The CCD Detector and the X-stage

The CCD detector is an area array of photo sensors. We use *InstaSpec IV* (Oriel, 1994). It consists of an CCD sensor chip *EEV 15-11*. The sensor chip is in 256 (row) × 1024 (column) pixel format. Each pixel size is 27 μm square. One whole row (1024 pixels) of the pixels can be read out at the same time. During operation, the CCD can be cooled to a low temperature to reduce dark current. Although dark current is unavoidable, it can be suppressed through low level by temperature control. In general, for every temperature rise of 5~7°C, the dark current doubles. Therefore, for keeping the operating temperature as low as possible, we can minimize the effect of dark current. Without cooling liquid, the CCD sensor can be cooled down to -5°C by air. If 10°C water is adopted for cooling, the temperature of the CCD sensor can be brought down to as low as -20~-28°C.

The spectral signal detected by the CCD is converted into digital data by a 16-bit A/D converter. Therefore, the dynamic range can be up to 65535 levels. The CCD detector has an interface card to transmit the data. It uses a 20 Hz clock to transmit the shift register (1024 pixels) data at one time. The interface is an ISA-based card as shown in Fig. 4. To obtain noise immunity, the spectral signal is sent through a coaxial cable.

For multispectral imaging, whiskbroom and pushbroom scanning mechanisms are frequently adopted to obtain the spatial dimensions of an image (Vane *et al.*, 1983; Goetz *et al.*, 1989; Diner *et al.*, 1989; Salomonson *et al.*, 1989; Neville *et al.*, 1995; Yamamoto *et al.*, 1996). Developments in solid-state array detectors and new optical spectroscopic components have further made it possible to achieve high precision and high spatial resolution results. In our design, since one of the dimensions of the area array CCD is used to pick up the radiance of spectra, to obtain the second spatial dimension of the image, a scanning mechanism is constructed by moving the object with a X-stage. The X-stage (Parker Hannifin Co.) is driven by a microstep motor. The characteristics of this X-stage is its convenient control interface and language syntax. It uses standard RS-232 for communications. The finest step is 10 nm. It is adjusted to give 50800 steps for each revolution. Before operating this device, the desired distance, velocity and direction must be set appropriately. The acceleration can also be programmed, but this is not necessary in this application.

III. Design of the Operating Software

Figure 5 shows a block diagram which indicates

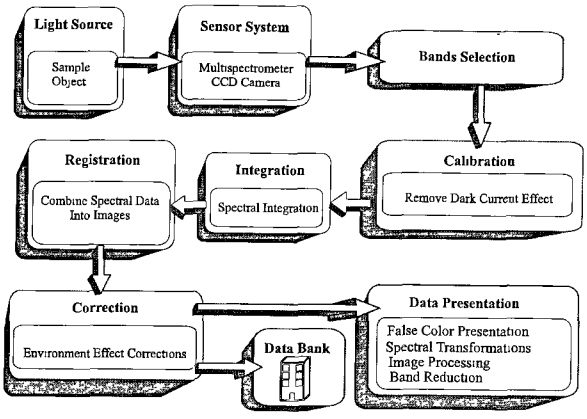

Fig. 5. A block diagram of the setup.

all the required operations of the multispectral imaging spectrometer. The light source delivers radiation from the visible to the near-infrared range. The major functions of the sensor system are to disperse radiation and to measure the intensity of each waveband. The desired number of wavebands is application dependent and can be up to 1024 bands. Therefore, a band selection function is used to choose the required wavebands and bandwidths. The programmable bandwidth is obtained by integrating pixels in the direction of the wavelength. The calibration function removes noise, such as dark current, of the CCD from the observed data. The registration function reconstructs the data obtained by pushbroom scanning into images, and then correction of environmental effects can be done on the image. Finally, spectral images are saved in a data bank for presentation and further application. Presentation of the spectral images in gray-scale, 16-color, and artificial RGB-color schemes is provided.

Figure 6 shows the principle of multispectral imaging. The radiation which is reflected by the area of interest of the sample object is dispersed

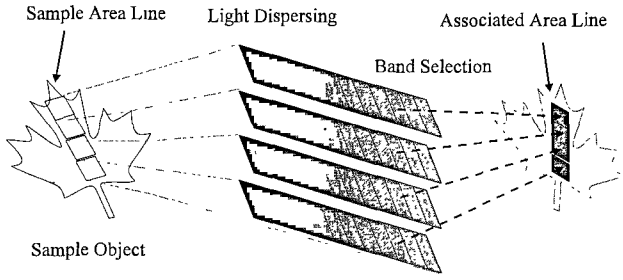

Fig. 6. Principle of multispectral imaging.

into many different wavebands by the monochromator. After choosing the desired wavebands, the appropriate spectra which go through the slit are measured by the CCD detector. The slit in the direction of height is mapped to the CCD in 256 instantaneous fields of view (IFOV), and the radiation observed by each IFOV is further dispersed into 1024 spectral bands. As a whole, a slit image is composed of 256×1024 CCD pixels. The pushbroom mechanism is constructed by means of slit imaging and X-stage scanning. The X-stage moves linearly so that the area of interest of the sample object can be brought line by line into the field of view through the slit. The spatial resolution on the sample object is determined mainly by using the IFOV, focal length and slit width. Figure 7 presents the complete process of taking spectral images. In order to make the process of taking spectral images as easy as possible, software has been developed to take care of the shaded blocks shown in Fig. 7.

The operating software can enable the user to avoid doing time consuming programming and setup. The whole idea is that the user does not need to take care of technical details, such as movement of the X-stage, programming of the CCD camera and so on. Adjustment of the slit width and the optical lens are the only required work on the hardware.

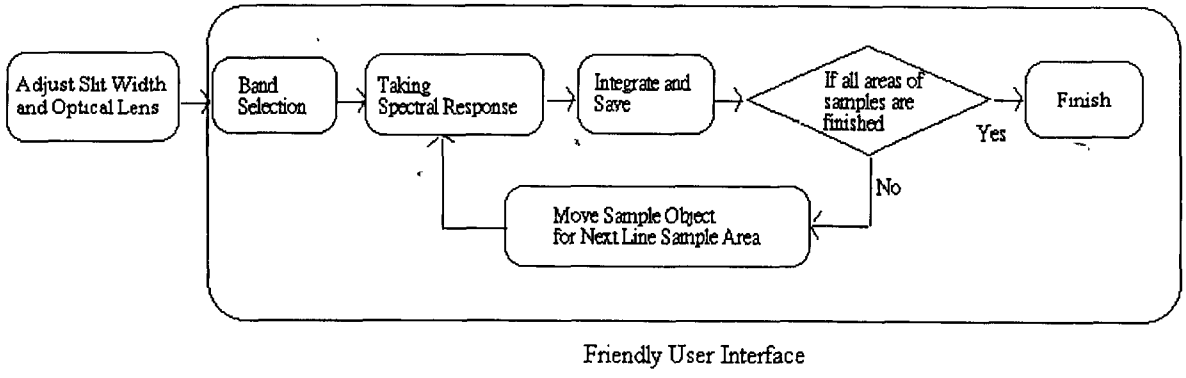

Fig. 7. Process of taking spectral images.

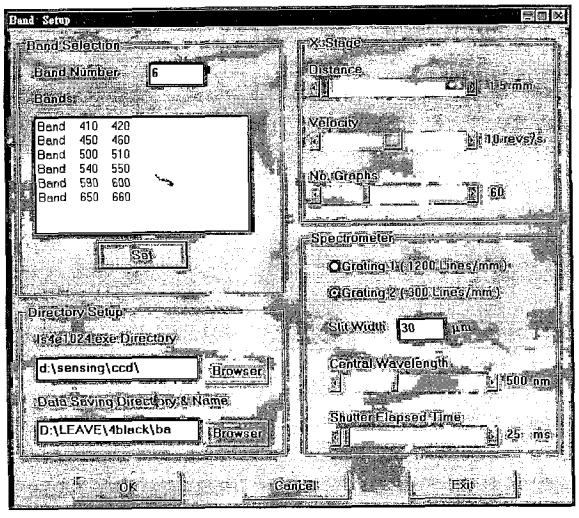

Fig. 8. The Band Setup window.

Everything else, including band selection and many other functions, can be finished by checking and answering the messages shown on the monitor. All physical actions are automatically controlled by the operating software. The operating software is installed on a personal computer running WINDOWS-95 (Microsoft Co.). An important advantage of using WINDOWS-95 is that it offers visual objects and compatibility with DOS (Disk Operating System). DOS is requested by the operating software when direct commands to the monochromator, CCD detector, and X-stage are required. The commands, feedback status and data are routed through a hardware dependent driver (Is4e1024.exe) under DOS. All the commands are fully supervised by the operating software. However, during execution of the driver software, the operating software switches automatically between WINDOWS-95 and DOS from time to time.

One of the commands for the monochromator is to note the grating and central wavelength selections. The CCD detector must be commanded to select the wavebands of interests, including each central wavelength and the corresponding bandwidth for integration. Figure 8 shows an example of setting up the wavebands. Moreover, commands for data transmission and triggering of the shutter to block the entrance of incoming radiation are also required. The time interval of shutter opening should be chosen appropriately to prevent the CCD detector from becoming saturated. The commands for the X-stage concern movement to finish the scanning procedure. The resulting spectral images can be displayed in any of the three color schemes: gray-scale, 16-color, and false RGB-color. For 16-color, the intensity of the spectral data is divided into 16 levels, and each level is displayed in a different color. For gray-scale, the intensity is presented in 256 gray levels. The artificial RGB-color shows three wavebands simultaneously. The three selected wavebands displayed correspond to red, green, and blue, respectively.

IV. Experimental Results

In this section, the multispectral imaging spectrometer was tested by observing two sample objects. The first one was used to test the geometric property. The second one was a leaf with green, brown and yellow regions to show the spectral characteristics. Section IV.1 shows the experimental arrangements. Section IV.2 presents the observation results for the first object. Section IV.3 gives the results of the leaf experiment.

1. Arrangement of the Experiments

Figure 9 shows the arrangement of the experimental system. The distance from the sample object to the focal plane determines the size of the scanning area. In the experiments, this distance was fixed to an appropriate value. The scanning performed by the X-stage was set to have a step size which matched the footprint of the slit width on the object plane. Since the light source is not collimated, the intensity is proportional to the inverse of the square of the distance. To avoid glitter, the monochromator and the light source are put on the same side of the object.

2. Geometric Property

To test the system in scanning and reconstruction of the image, a sample object as shown in Fig. 10 was

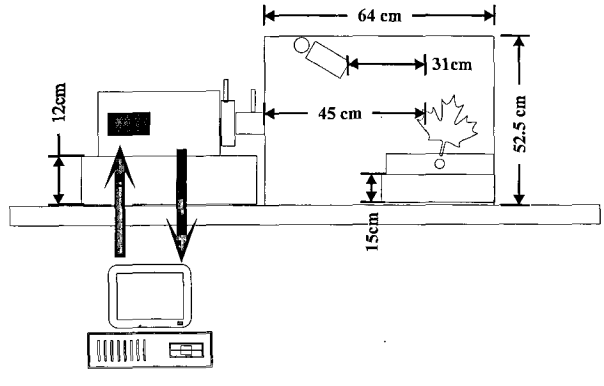

Fig. 9. Experimental arrangement.

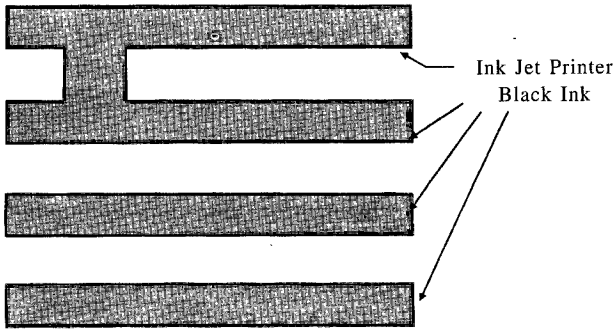

Fig. 10. A geometric image (true RGB-color).

used. The geometric image was plotted by using two different kinds of inks. Four horizontal black lines were printed by an ink-jet printer. Between the first and second black lines, there was a block which was made using a black marker pen. Black was chosen because it could be easily observed by the spectrometer in most of the wavebands.

The first step of the experiment was to set up suitable bands for observation. Figure 8 shows the band setup window. In this experiment, the X-stage movement was 1.5 mm per step, and it moved for 60 steps. We selected 6 bands and used grating 2 (300 lines/mm). The central wavelength of the monochromator was set to 500 nm. The slit width was 30 mm. The shutter elapse time was 25 ms.

Figures 11-13 show the experimental results obtained using the above settings. In Fig. 11, the spectral image has a waveband of 410~420 nm. All the black lines can be clearly identified in the images. Comparing Fig. 11 with Fig. 10, the major difference is the line edge. In Fig. 11, the line edge is blurry in the horizontal direction, but this isn't the case in the vertical direction. Mechanical scanning and image reconstruction could cause blurring in the horizontal direction, but because the CCD pixels abutted each other, the resolution in the vertical direction was much better.

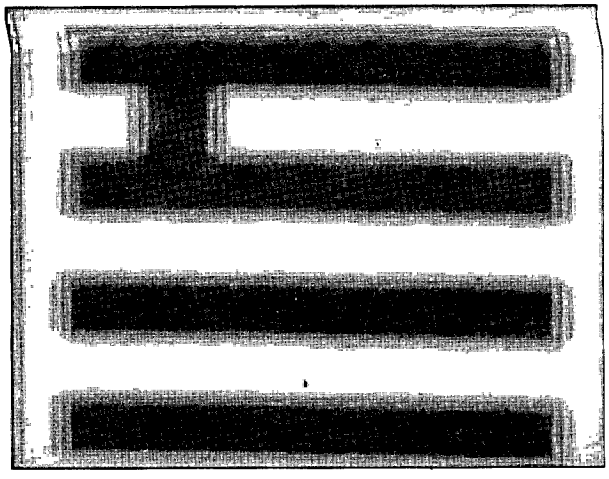

Fig. 11. Band 410~420 nm (gray-scale).

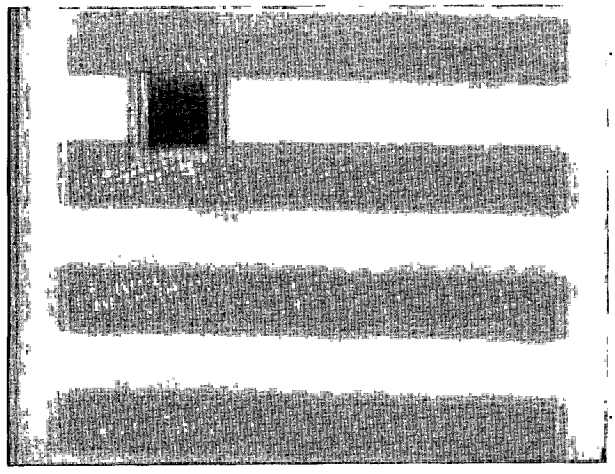

Fig. 12. Band 590~600 nm (gray-scale).

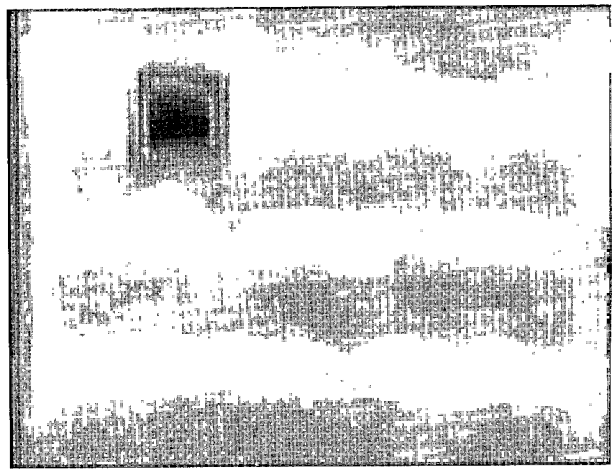

Fig. 13. Band 650~660 nm (gray-scale).

The spectral image shown in Fig. 12 was taken with a 590~600 nm waveband. The four black lines produced by the ink jet printer have become blurred, but the block made using the marker pen is the same as in Fig. 11 except a little bit brighter. This shows that the black lines had weaker reflection in band 590~600 nm. When the wavelength increased, the difference became more obvious. Figure 13 shows the result using band 650~660 nm. The black lines are much weaker, and this clearly shows the difference in the ink.

3. The Leaf Experiment

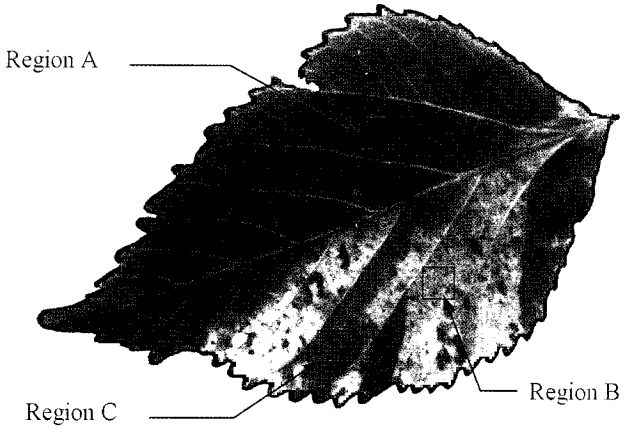

Fig. 14. A leaf sample (true RGB-color).

A color photo of the leaf sample is shown in Fig. 14. On the leaf, more than three colors can be seen. To determine the wavebands for observation, we first took the spectral signature curves for the sample in different regions. A sheet of white paper with three square holes in it was used to mask the leaf. The holes were the regions of the leaf to be observed for spectral signature curves. In Fig. 14, region A represents the darker area of the leaf. This color was close to dark green or brown. Region B represents the brightly colored area of the leaf. This color was close to bright red. Region C represents the dark red color, which was brighter than dark green. Every region was the same size in height and width. The monochromator was adjusted so as to focus on the target to get the spectral signature curves. The results are shown in Fig. 15. Figure 16 shows the normalized intensities of the reflections. It is found that the spectral signature curve decayed a lot in 300~600 nm, but the difference in the reflection between region A and region B, as shown in Fig. 17, increased rapidly in 420~540 nm. This means that 420~540 nm was suitable for classifying region A and region B. Because of unavoidable noise,

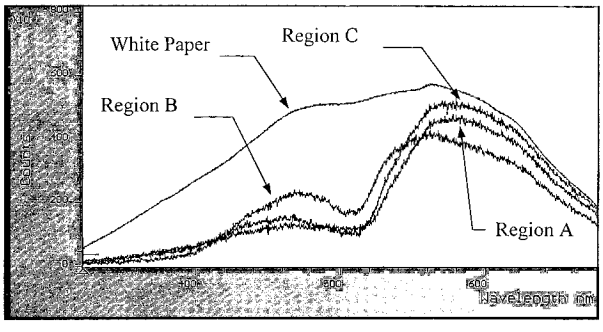

Fig. 15. Spectral signature curves.

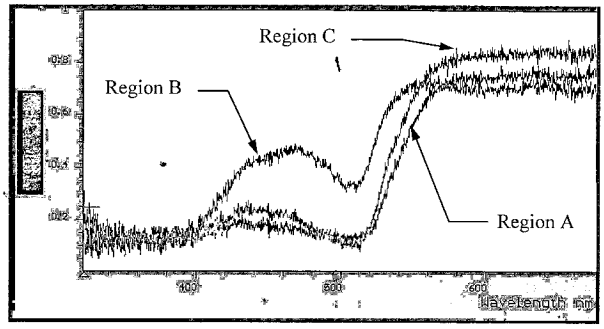

Fig. 16. Normalized reflection intensities.

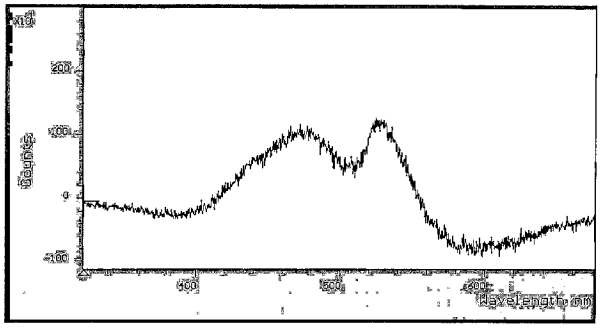

Fig. 17. The difference between two spectral signature curves (B-A).

the values in Fig. 17 vary about 50 counts. Based on the above results, we can choose wavebands of interest for observation. The Band Setup window is shown in Fig. 18.

In order to improve the resolution in the horizontal direction, the step size of the X-stage was set to

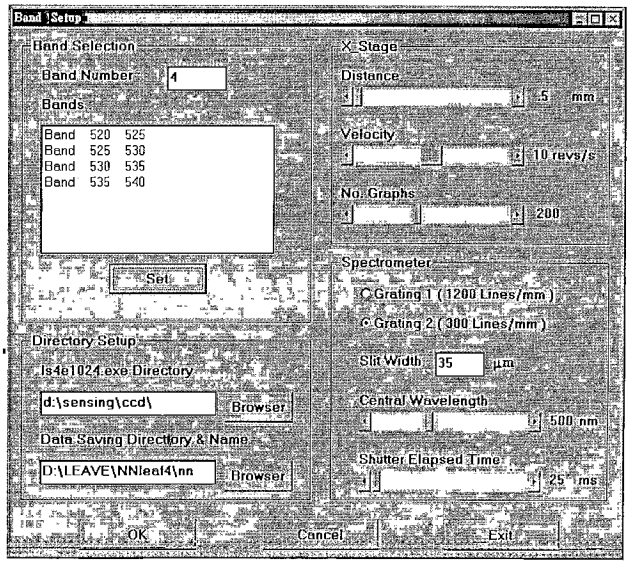

Fig. 18. Band Setup window for leaf example.

0.5 mm, the number of graphs (steps) to 200, and the slit width to 35 μm. Four concatenate wavebands, 520~525 nm, 525~530 nm, 530~535 nm, and 535~540 nm were selected to investigate the spectral range of rapid reflection change. After completing the setup, we started the imaging spectrometer and observe a spectral image of the selected bands. Figures. 19-21 show the spectral images of three bands in the gray-scale and 16-color schemes, respectively. Figure 19(a) shows the gray-scale image. The intensity is divided into 256 gray levels from bright to dark. The dark and bright parts of the leaf can be clearly identified in the image. Comparing with the original leaf as shown in Fig. 14, the dark part corresponds to the dark green region of the leaf. The bright part is the red region of the leaf. The venation of the leaf can also be identified in the image, but is not so clear. Figure 19(b) shows the distribution of the reflective intensity obtained using 16-color scheme.

Figures 20 and 21 show the spectral images of the other two bands with longer wavelengths. The color schemes are the same as in Fig. 19. Comparing with Fig. 19, stronger reflection is found in these bands. It is possible to clearly discriminate the venation from the other regions of the leaf.

To show the programmable ability of wavebands, the imaging spectrometer was applied to observe the leaf using the six wavebands of the Ocean Color Imager (OCI). OCI is a payload of the ROCSAT-1 satellite sponsored by National Science Council to observe ocean pigments. It is scheduled to be launched in 1998. Table 1 shows the wavelengths of the six wavebands. Figure

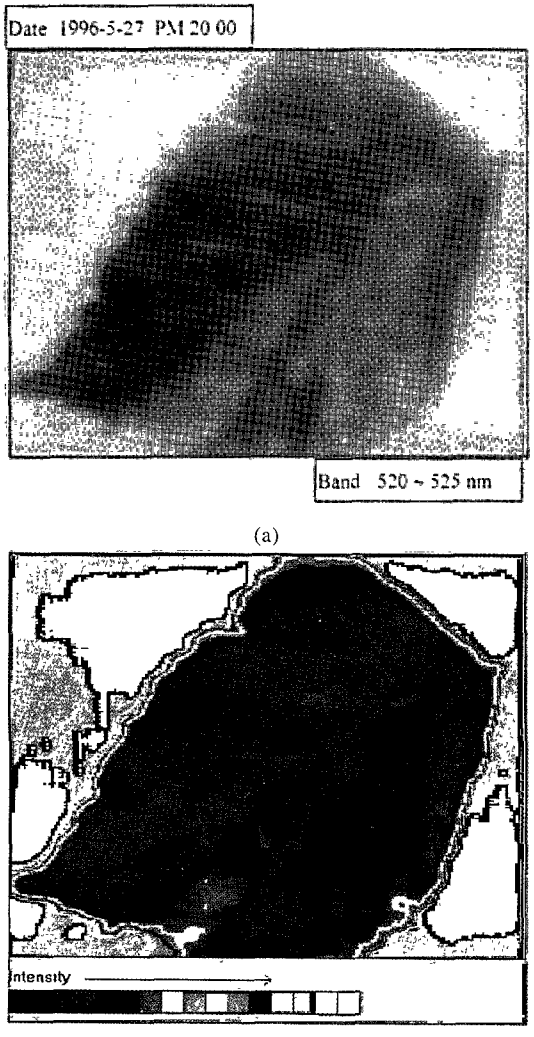

Fig. 19. Images of band 1 (520~525 nm), (a) 256 gray levels, (b) 16-color.

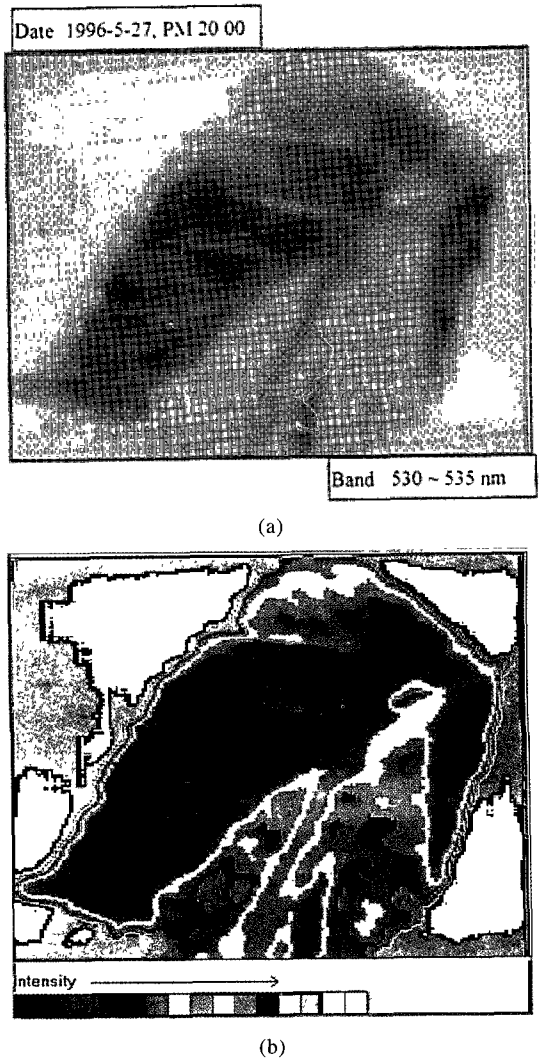

Fig. 20. Images of band 3 (530~535 nm), (a) 256 gray levels, (b) 16-color.

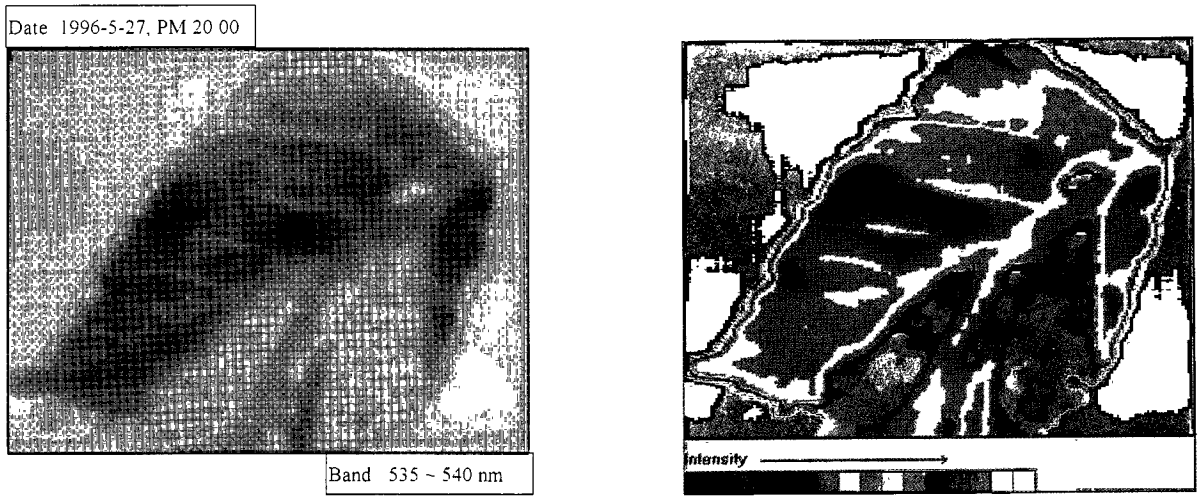

(a) (b)

Fig. 21. Images of band 4 (535~540 nm), (a) 256 gray levels, (b) 16-color.

Table 1. Wavebands of the OCI

OCI wavebands	
band 1	433 ~ 453 nm
band 2	480 ~ 500 nm
band 3	500 ~ 520 nm
band 4	545 ~ 565 nm
band 5	660 ~ 680 nm
band 6	845 ~ 885 nm

22 shows the six gray-scale images of the leaf observed by the imaging spectrometer. From previous study of the leaf, it was known that the leaf had strong absorption from wavelength 400 nm to 540 nm. Therefore, Fig. 22 (a)-(c) depict the dark images of band 1, band 2, and band 3. The bright images in Fig. 22 (d) and (e) show that the leaf had strong reflection in Bands 4 and 5. The absorption in Band 6 resulted from the water content of the leaf. Figure 23 used the artificial RGB-color scheme to present the results. Each image shows three wavebands. Presentation by artificial RGB-color can dye the image so that the characteristics of interest may appear significantly. Certainly except presenting the results by gray-scale or color images, the spectral data could be saved in a data bank of the imaging spectrometer for further study.

VI. Conclusion

In this research we have successfully built a multispectral imaging spectrometer with programmable wavebands for investigation of the spectral signatures of sample objects. The spectral range of detection was from 400 nm to 900 nm, which covered all six wavebands of OCI. A pushbroom mechanism was applied to scan the sample object for an area as large as 10 cm square. The resolution across the track direction was 256 CCD-pixels whereas along the track, the finest scanning motion was as small as 10 nm. The wavebands of interest, including number and bandwidth, were programmable. In the extreme case, 1024 wavebands, 0.1 nm bandwidth and 16-bit resolution of intensity could be achieved. For immediate display of the spectral images, 16-color, gray-scale, and false RGB-color schemes were used to enhance the presentation. The whole system was tested by investigating the spectral responses of two sample objects. The geometric pattern sample confirmed the excellent spatial features of the multispectral imaging spectrometer. The leaf imaging experiment demonstrated the ability of the system in band selection and in identifying spectral signatures at different locations of an object. In the near future, further improvement using a collimated light source to mimic passive remote sensing will be implemented. More advanced calibration, correction and registration functions will be built into the processing software for interpretation of observed spectral images.

Acknowledgment

Financial support for this research from the National Science Council, R.O.C., under contract NSC 85-2612-E002-001 and equipment support from the National Space Program Office of Taiwan, R.O.C., under OCI project are gratefully acknowledged.

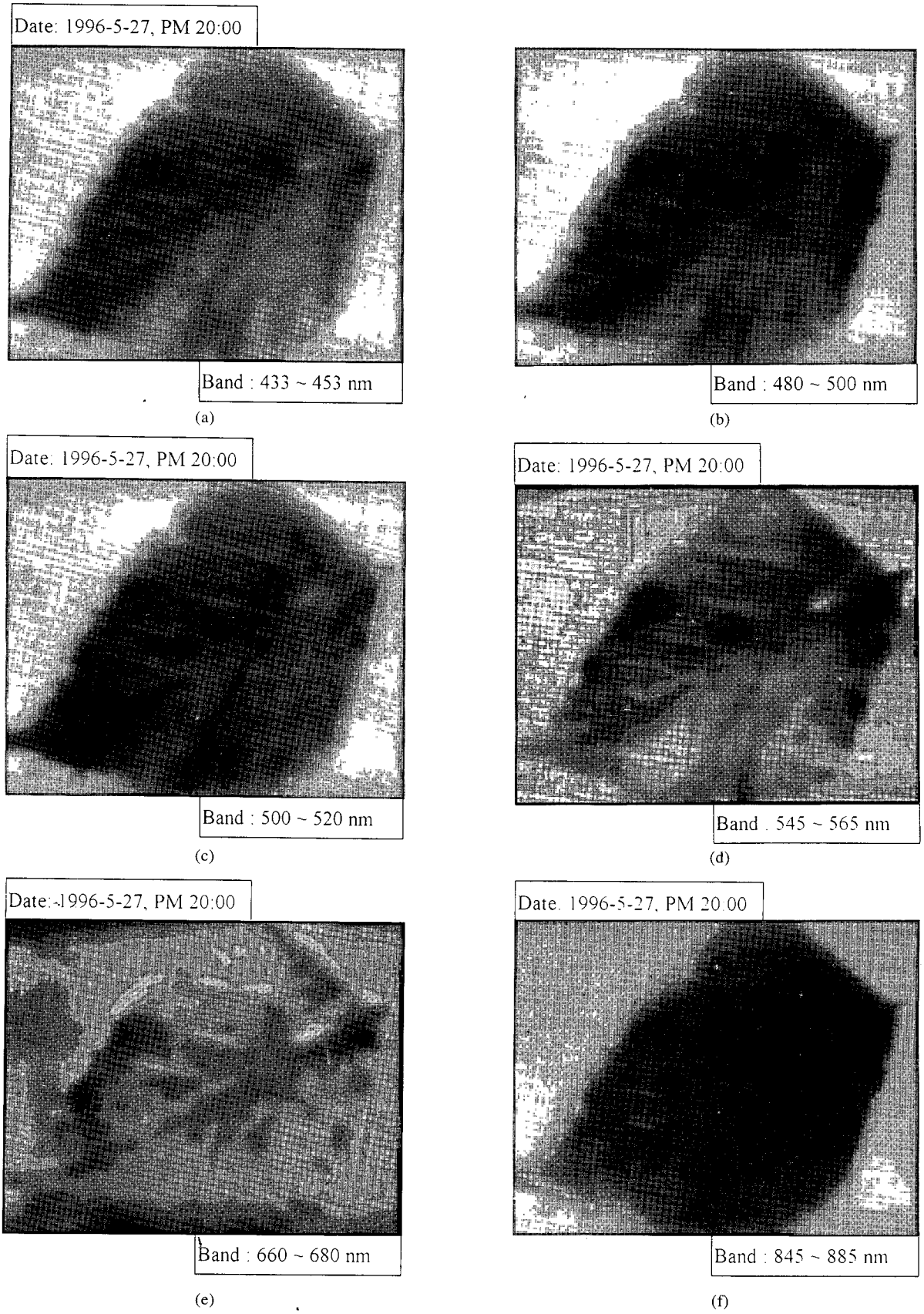

Fig. 22. Gray-scale images of the leaf in OCI bands. (a) Band 1. (b) Band 2. (c) Band 3. (d) Band 4. (e) Band 5. (f) Band 6.

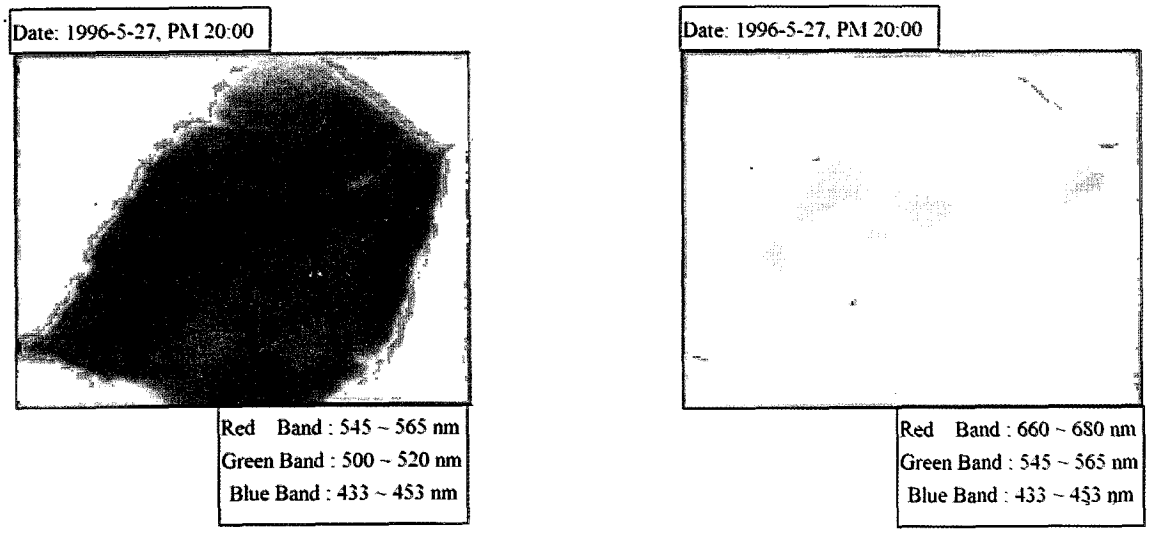

Fig. 23. (a) Artificial RGB-color representation of three bands. (b) Artificial RGB-color representation of the other three bands.

References

Buschmann, C., E. Nagel, K. Szabó, and L. Kocsányi (1994) Spectrometer for fast measurements of in vivo reflectance, absorptance, and fluorescence in the visible and near-infrared. *Remote Sensing of Environment*, **48**, 18-24.

Diner, D. J., C. J. Bruegge, J. V. Martonchik, T. P. Ackerman, R. D. Siegfried, A. W. Gerstl, H. R. Gordon, P. J. Sellers, J. Clark, J. A. Daniels, E. D. Danielson, V. G. Duval, K. P. Kiaasen, G. W. Lilienthal, D. I. Naknmoto, R. J. Pagano, and T. H. Reilly (1989) MISR: a multiangle imaging spectroradiometer for geophysical and climatological research from EOS. *IEEE Transactions on Geoscience and Remote Sensing*, **27**(2), 200-211.

Elachi, C. (1987) *Introduction to Physics and Techniques of Remote Sensing*. John Wiley & Sons, Inc., New York, NY, U.S.A.

Goetz, A. F. H. and M. Herring (1989) The high resolution imaging spectrometer (HIRIS) for EOS. *IEEE Transactions on Geoscience and Remote Sensing*, **27**(2), 136-144.

Neville, R. A., N. Rowlandsm, R. Marois, and I. Powell (1995) SFSI: Canada's first airborne SWIR imaging spectrometer. *Canadian Journal of Remote Sensing*, **21**(3), 328-336.

Ning, L., G. E. Edwards, G. A. Strobel, L. S. Daley, and J. B. Callis (1995) Imaging fluorometer to detect pathological and physiological change in plants. *Applied Spectroscopy*, **49**(10), 1381-1389.

Oriel handbook (1994) *Light Sources, Monochromators and Spectrographs, Detectors and Detection Systems, Fiber Optics*. Vol. II, Ch. 2, pp. 20-23. Oriel Corporation, Stratford, CT, U.S.A.

Pomeroy, R. S., M. E. Baker, M. B. Denton, and A. G. Dickson (1995) Scientifically operated CCD-based spectroscopic system for high-precision spectrometric determinations of seawater. *Applied Spectroscopy*, **49**(12), 1729-1736.

Salomonson, V. V., W. L. Barnes, P. W. Maymon, H. E. Montgomery, and H. Ostrow (1989) MODIS: advanced facility instrument for studies of the Earth as a system. *IEEE Transactions on Geoscience and Remote Sensing*, **27**(2), 145-153.

Vane, G., A. F. H. Goetz, and J. B. Wellman (1983) Airborne imaging spectrometer: A new tool for remote sensing. *Proc. IEEE Int Geosci. Remote Sensing Symposium*, **Fa-4**, 6.1-6.5.

Yamamoto, K., D. A. Cremers, M. J. Ferris, and L. E. Foster (1996) Detection of metals in the environment using a portable laser-induced breakdown spectroscopy instrument. *Applied Spectroscopy*, **50**(2), 222-233.

Programmable Imaging Spectrometer

可選擇頻帶之多頻帶譜像儀

林巍聳　黃奇沛　蘇怡仁

國立台灣大學電機工程研究所

摘　要

偵測實物樣本的頻譜特性，是選定遙測頻帶與判讀遙測結果所必須的。針對這個目的，本研究發展出一套可因應不同的應用需求、調整偵測頻帶數目與帶寬的多頻帶譜像儀，實際製作完成的多頻帶譜像儀，可以偵測400奈米（nm）到900奈米的波長，涵括可見光與近紅外光的範圍，也涵括未來中華一號衛星上，海洋水色儀的所有六個頻帶。本多頻帶譜像儀，用一個平面型電藕合感測器（CCD）、一個十六位元類比數位轉換器、以及推掃機制（pushbroom），構成強度、波長、影像長、影像寬等四度空間的偵測與顯像機能，應用的極限，可以達到1024個偵測頻帶、0.1 奈米的帶寬、16位元的強度解析能力、10平方厘米的偵測面積，整個系統主要包括分光器、電藕合感測器、白光源、線型平台、處理機等五個硬件，其整合操作與偵測、攝像，均由一套作業軟體自動負責監控，所取得的頻譜數據，可以立即顯像，也可以儲存起來，以供後續研究之用。顯像時，可以選用灰階、十六色、或紅綠藍假色以加強效果。爲測試與展現本多頻帶譜像儀的性能，論文中詳實的記錄了一個幾何樣本和一個樹葉樣本的譜像偵測結果，其中也有用海洋水色儀的六個頻帶所偵測得的譜像。